Post-print of: Z. Kowalczuk and M. Tatara, "Analytical Steady-State Model of the Pipeline Flow Process," 2018 23rd International Conference on Methods & Models in Automation & Robotics (MMAR), Miedzyzdroje, 2018, pp. 182-187, doi: 10.1109/MMAR.2018.8486066.

Analytical Steady-State Model of the Pipeline Flow Process

Zdzisław Kowalczuk
Department of Robotics and Decision Systems
Faculty of Electronics, Telecommunications and Informatics
Gdańsk University of Technology
ul. Narutowicza 11/12, 80-233 Gdańsk, Poland
Email: kova@pg.edu.pl

Marek Tatara
Department of Robotics and Decision Systems
Faculty of Electronics, Telecommunications and Informatics
Gdańsk University of Technology
ul. Narutowicza 11/12, 80-233 Gdańsk, Poland
Email: martatar@pg.edu.pl

***Abstract*—The paper addresses the issue of modeling the flow process in transmission pipelines. A base model used for numerical simulation is introduced. Under certain assumptions concerning steady state analysis, the differential equations describing the process are solved analytically for two cases: zero and nonzero inclination angle α. These equations describe a constant flow rate and a corresponding distribution of the pressure along the considered pipeline for both cases. The pipe length at which the pipeline is choking (the mass flow is equal zero) for given boundary pressures and inclination angle, is also derived. Convergence of the proposed solution for inclination angle $\alpha \to 0$ to the zero tilt solution, is proved. An exemplary practical relationship based on obtained equations is provided as a 3D chart. A test pipeline with adjustable inclination angles of its selected parts is considered. The analytic solution for the effective angle is compared with numerical solutions, which show relevant discrepancies between the results obtained for nonzero angles. Clearly, the numerical solution for a straight pipeline (with the increasing number of segments) is convergent to the analytic solution. Moreover, up to 16°, the analytic approximation (using an effective inclination angle) is sufficient, and produces similar results as the numerical simulation.**

I. Introduction

Modeling of flow processes in transmission pipelines allows theoretically studying the behavior of transported fluids and practically detecting leakages in pipeline installations; what can be used to quickly react to such leaks using respective model-based leak detection and localization systems. For example, based on measurements gained from pressure and flow sensors at the inlet and outlet of a pipeline, relevant state-space observers can estimate intermediate fluid parameters that produce some residual signals that, after further processing, provide a basis for leakage detection and isolation (LDI).

Eearly application of nonlinear state observers to the detection and identification of a single leak in a pipeline can be found in the literature [1], [3], [4], for instance. Multiple-leak detection is considered in [2], [13], while an interesting extension of the LDI problem towards branched pipelines is proposed in [14]. Not-model-based approaches can be based, for instance, on the pressure wave propagation analysis in the time domain [12], the acoustic wave cross time-frequency spectrum analysis [9], [10] or the rough set theory and support vector machines [11].

Practical model-based leak detection systems require a mathematical description suitable for numerical simulation of fluid flow on field computers. Therefore, the problem of limited computational resources arises, which motivates our investigation aimed at reduction of the computational overhead in simulations of the flow process in transmission pipelines.

II. Base Model of the Flow Process

Let us consider the principal mathematical description of the pressure and mass-flow rate of liquid flowing in a transmission pipeline, which is expressed by the following two equations, resulting from the momentum and mass conservation laws [1]:

$$\frac{A}{\nu^2}\frac{\partial p}{\partial t} + \frac{\partial q}{\partial z} = 0 \tag{1}$$

$$\frac{1}{A}\frac{\partial q}{\partial t} + \frac{\partial p}{\partial z} = -\frac{\lambda \nu^2}{2DA^2}\frac{q|q|}{p} - \frac{gsin\alpha}{\nu^2}p \tag{2}$$

where A is the cross-sectional area $[m^2]$, ν is the isothermal velocity of the sound in the fluid $[\frac{m}{s}]$, D is the diameter of the pipe $[m]$, q is the mass flow $[\frac{kg}{s}]$, p is the pressure $[Pa]$, t is the time $[s]$, z is the spatial coordinate $[m]$, λ is the dimensionless generalized friction factor, α is the inclination angle $[rad]$, and g is the gravitational acceleration $[\frac{m}{s^2}]$.

Since the operation of a model-based algorithm for pipeline diagnosis usually requires simulation of the behavior of the underlying flow process, the set of equations (1)–(2) is discretized in order to enable computer implementation. In such cases, the pipeline is divided into N segments of equal length Δz, where the pressure at the end of each odd segment, and the flow rate at the end of each even segment, are the main object of calculations. The resulting mass-flow and pressure are computed at the inlet and outlet of the pipeline, as well. A diagram of such a discretized pipeline is represented in Fig. 1.

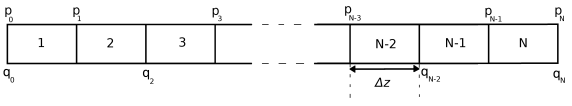

Fig. 1. Discretization scheme of a pipeline with N segments

The discrete-time model is developed by properly inserting low-order central difference schemes [1]:

$$\frac{\partial x}{\partial t} = \frac{3x_d^{k+1} - 4x_d^k + x_d^{k-1}}{2\Delta t} \tag{3}$$

$$\frac{\partial x}{\partial z} = \frac{x_{d+1}^{k+1} - x_{d-1}^{k+1} + x_{d+1}^k - x_{d-1}^k}{4\Delta z} \tag{4}$$

where Δz is a spatial-step size, Δt is a time-step size, subscripts and superscripts stand for the number of the pipeline segment and discrete-time index, respectively.

By implementing (3)–(4) in the composed model (1)–(2), one obtains the following state-space representation:

$$\mathbb{A}\hat{\mathbf{x}}^k = \mathbb{B}\hat{\mathbf{x}}^{k-2} + \mathbb{C}\left(\hat{\mathbf{x}}^{k-1}\right)\hat{\mathbf{x}}^{k-1} + \mathbb{D}\mathbf{u}^{k-1} + \mathbb{E}\mathbf{u}^k \tag{5}$$

Taking into account nonsingularity of $\mathbb{A}$, the so-called recombination matrix [5], [7], [8], one obtains:

$$\hat{\mathbf{x}}^k = \mathbb{A}^{-1}\left(\mathbb{B}\hat{\mathbf{x}}^{k-2} + \mathbb{C}\left(\hat{\mathbf{x}}^{k-1}\right)\hat{\mathbf{x}}^{k-1} + \mathbb{D}\mathbf{u}^{k-1} + \mathbb{E}\mathbf{u}^k\right) \tag{6}$$

where $\mathbb{B}$ and $\mathbb{C}\left(\hat{\mathbf{x}}^{k-1}\right)$ are associated with the nonlinear dynamics of the above system state

$$\hat{\mathbf{x}}^k = \left[\begin{array}{cccc|cccc} q_0^k & q_2^k & q_4^k & \cdots q_N^k & p_1^k & p_3^k & p_5^k \cdots & p_{N-1}^k \end{array}\right]^T \in \mathbb{R}^{N+1}$$

and matrices $\mathbb{D}$ and $\mathbb{E}$ are associated with the input $\mathbb{u}^k = \left[\begin{array}{cc} p_0^k & p_N^k \end{array}\right]^T \in \mathbb{R}^2$. A full description of these matrices can be found in [7].

III. Analytic Solution of the Flow Equations for Steady State

The solution will be provided for two separate cases: when the inclination angle is zero or nonzero. The division allows us to simplify the solution for $\alpha = 0$. The convergence between the two cases will also be analyzed. In both cases we start with the following two differential equations describing all flow processes:

$$C_1\frac{\partial p}{\partial t} + \frac{\partial q}{\partial z} = 0 \tag{7}$$

$$C_2\frac{\partial q}{\partial t} + \frac{\partial p}{\partial z} = -C_3\frac{q|q|}{p} - C_4 p \tag{8}$$

where $C_1 = \frac{A}{\nu^2}$, $C_2 = \frac{1}{A}$, $C_3 = \frac{\lambda\nu^2}{2DA^2}$, $C_4 = \frac{gsin\alpha}{\nu^2}$

Let us assume that the LDI system works for a pipeline with steady flow, that is, the pressure and flowrate remain unchanged in time. Then, even for small changes in the inlet or outlet pressure measured by sensors (e.g. resulting from sensor outliers or non-stationary work of the pumping system), this assumption means that the whole characteristics along the pipeline can be calculated according to given boundary conditions (for any computational moment, in this steady state). Therefore, we consider $\frac{\partial q}{\partial t} \to 0$ and $\frac{\partial p}{\partial t} \to 0$ as approximately satisfied for steady flow. In such cases, the partial differential equations reduce to ordinary differential equations. We propose here the simplified denotations p and q, hiding their functional dependence on the space, $p(z)$ and $q(z)$, which represent the description of the pressure and mass-flow for any spatial coordinate z along the length of the considered pipeline.

A. Zero Inclination Angle, $\alpha = 0$

In the case of the zero inclination angle, the system of equations describing the flow process, under the previously specified assumptions about steady state ($\frac{\partial q}{\partial t} \to 0$ and $\frac{\partial p}{\partial t} \to 0$), can be, due to $C_4 = 0$, further simplified to:

$$\frac{dq}{dz} = 0 \tag{9}$$

$$\frac{dp}{dz} = -C_3\frac{q|q|}{p} \tag{10}$$

The flow rate is thus constant in space (as described by (9)) and in time (as results from the steady-state assumption). By introducing $C_3'(q) = C_3 q|q|$, the second equation can be shown as

$$p\frac{dp}{dz} = -C_3'(q) \tag{11}$$

Integrating both sides of the equation

$$\int p dp = \int -C_3'(q) dz \tag{12}$$

leads to

$$p^2 = -2C_3'(q)z + C \tag{13}$$

For unknown mass flow, with the aim of determining the two unknown constants C and $C_3'(q)$, we introduce two boundary conditions $p_i = p(z)|_{z=0}$ and $p_o = p(z)|_{z=L}$, where p_i and p_o are the measurements of the input and output pressures, respectively. Substituting the first boundary condition to (13) immediately leads to

$$C = p_i^2 \tag{14}$$

The second boundary condition is used to determine the value of $C_3'(q)$, and indirectly, the value of q. Substituting $p_o = p(z)|_{z=L}$ into (13) yields

$$p_o^2 = -2C_3'(q)L + p_i^2 \tag{15}$$

which leads to

$$C_3'(q) = \frac{p_i^2 - p_o^2}{2L} \tag{16}$$

Therefore,

$$q|q| = \frac{DA^2}{\lambda\nu^2}\frac{p_i^2 - p_o^2}{L} \tag{17}$$

Note that the mass-flow rate sign depends on the sign of the difference $p_i^2 - p_o^2$ (other parameters are positive). If the inlet pressure is higher than the outlet pressure, the fluid flows from the default input to the output. If, however, the inlet pressure is lower, the fluid flows into the opposite direction (this will give you a minus sign). Taking this into account, we can determine

$$q = sign\left(p_i^2 - p_o^2\right)\sqrt{\left|\frac{DA^2}{\lambda\nu^2}\frac{p_i^2 - p_o^2}{L}\right|} \tag{18}$$

where $sign(x)$ is 1 for $x \geq 0$, and -1 otherwise. The known integration constant C and parameter $C_3'(q)$ can now

be implemented in (13), which after rearranging leads to the following pressure distribution along the line:

$$p = \sqrt{p_i^2 - \frac{p_i^2 - p_o^2}{L} z} \tag{19}$$

The last two equations allow us to compute the mass-flow rate and pressure distribution along the pipe for given physical properties of the flow process. Hence, one can calculate the values of the corresponding parameters; for instance, the pipe length required for a specific mass-flow rate (with other parameters fixed) or the friction factor for measured flow and pressure.

B. Nonzero Inclination Angle

Now, taking into account the original set of equations (7)-(8) and a nonzero inclination angle, along with the aforementioned steady state conditions, we have

$$\frac{dq}{dz} = 0 \tag{20}$$

$$\frac{dp}{dz} = -C_3 \frac{q|q|}{p} - C_4 p \tag{21}$$

From (20) we have an immediate result $q(z) = const$. Thus, only (21) remains unsolved. Again, for a constant q, let us consider using the auxiliary parameter $C_3'(q) = C_3 q|q|$. Rewriting equation (21) leads to

$$\frac{dp}{dz} = -C_3'(q) p^{-1} - C_4 p \tag{22}$$

Dividing it by the right-hand side and changing the sign of both sides results in

$$\frac{1}{C_3'(q) p^{-1} + C_4 p} \frac{dp}{dz} = -1 \tag{23}$$

which, by separation of the variables, is equivalent to

$$\frac{p}{C_3'(q) + C_4 p^2} dp = -dz \tag{24}$$

Note that according to (20) we can assume that $C_3'(q)$ is z-invariant, thus, integrating both sides of (24) gives

$$\frac{1}{2C_4} ln(C_4 p^2 + C_3'(q)) = -z + C \tag{25}$$

where C is an integration constant. Note that (25) is sure to exist for $C_4 \neq 0$ (which is equivalent to nonzero inclination angle). Now we substitute boundary conditions $p(z)|_{z=0} = p_i$ and $p(z)|_{z=L} = p_o$ to calculate the values of the integration constant and the other unknown coefficient $C_3'(q)$. First, for $z = 0$ we have the integration constant

$$C = \frac{1}{2C_4} ln(C_4 p_i^2 + C_3'(q)) \tag{26}$$

Since $C_4 = \frac{gsin\alpha}{\nu^2}$, the following solution can be safely applied for these segments of the pipeline which have their inclination angle non-zero. Therefore, putting this constant into (25) leads to the following development

$$\frac{1}{2C_4} ln(C_4 p_o^2 + C_3'(q)) = -L + \frac{1}{2C_4} ln(C_4 p_i^2 + C_3'(q)) \tag{27}$$

$$ln\left(C_4 p_i^2 + C_3'(q)\right) - ln\left(C_4 p_o^2 + C_3'(q)\right) = 2C_4 L \tag{28}$$

$$ln\left(\frac{C_4 p_i^2 + C_3'(q)}{C_4 p_o^2 + C_3'(q)}\right) = 2C_4 L \tag{29}$$

$$\left(\frac{C_4 p_n^2 + C_3'(q)}{C_4 p_o^2 + C_3'(q)}\right) = e^{2C_4 L} \tag{30}$$

$$\left(C_4 p_i^2 + C_3'(q)\right) = C_4 p_o^2 e^{2C_4 L} + C_3'(q) e^{2C_4 L} \tag{31}$$

$$C_4 p_i^2 - C_4 p_o^2 e^{2C_4 L} = C_3'(q) e^{2C_4 L} - C_3'(q) \tag{32}$$

$$C_4\left(p_i^2 - p_o^2 e^{2C_4 L}\right) = C_3'(q)\left(e^{2C_4 L} - 1\right) \tag{33}$$

$$C_3'(q) = C_4\left(\frac{p_i^2 - p_o^2 e^{2C_4 L}}{e^{2C_4 L} - 1}\right) \tag{34}$$

which is the sought parameter. However, as $C_3' = \frac{\lambda \nu^2}{2DA^2} q|q|$, we can now compute the flowrate from

$$q|q| = \frac{2DA^2}{\lambda \nu^2} C_4\left(\frac{p_i^2 - p_o^2 e^{2C_4 L}}{e^{2C_4 L} - 1}\right) \tag{35}$$

which, by keeping in mind the proper sign of flow and using the $sign$ function, gives the result

$$q = \sqrt{\left|\frac{2DA^2}{\lambda \nu^2} C_4\left(\frac{p_i^2 - p_o^2 e^{2C_4 L}}{e^{2C_4 L} - 1}\right)\right|} sign\left(p_i^2 - p_o^2 e^{2C_4 L}\right) \tag{36}$$

Taking into account the value of C_4, we obtain the respective dependency of flow on the inclination angle α:

$$q = \sqrt{\left|\frac{2DA^2}{\lambda \nu^2} \frac{gsin\alpha}{\nu^2}\left(\frac{p_i^2 - p_o^2 e^{2\frac{gsin\alpha}{\nu^2} L}}{e^{2\frac{gsin\alpha}{\nu^2} L} - 1}\right)\right|} sign\left(p_i^2 - p_o^2 e^{2\frac{gsin\alpha}{\nu^2} L}\right) \tag{37}$$

Note that there may exist a determined point (for a given positive angle of inclination and pressure ratio) for which the flow is zero, i.e. $C_3'(q) = 0$. Using this result in (33) leads to

$$C_4\left(p_i^2 - p_o^2 e^{2C_4 L}\right) = 0 \tag{38}$$

$$p_i^2 = p_o^2 e^{2C_4 L} \tag{39}$$

$$\frac{gsin\alpha}{\nu^2} L = ln\left(\frac{p_i}{p_o}\right) \tag{40}$$

L, so determined, is the length at which the pipeline is choking ($q = 0$) for given pressure and tilt angle.

Now, for the computed constants, the pressure characteristics along the pipeline can be determined as follows:

$$\frac{1}{2C_4} ln(C_4 p^2 + C_3'(q)) = -z + \frac{1}{2C_4} ln(C_4 p_i^2 + C_3'(q)) \tag{41}$$

$$ln(C_4 p^2 + C_3'(q)) = -2C_4 z + ln(C_4 p_i^2 + C_3'(q)) \tag{42}$$

$$C_4 p^2 + C_3'(q) = e^{-2C_4 z}\left(C_4 p_i^2 + C_3'(q)\right) \tag{43}$$

$$p^2 = e^{-2C_4 z}\left(p_i^2 + \frac{C_3'(q)}{C_4}\right) - \frac{C_3'(q)}{C_4} \tag{44}$$

$$p^2 = e^{-2C_4 z} p_i^2 + \frac{C_3'(q)}{C_4}\left(e^{-2C_4 z} - 1\right) \tag{45}$$

By using (34) in the above, one obtains

$$p^2 = e^{-2C_4 z} p_i^2 + \left(\frac{p_i^2 - p_o^2 e^{2C_4 L}}{e^{2C_4 L} - 1}\right)\left(e^{-2C_4 z} - 1\right) \tag{46}$$

$$p = \sqrt{e^{-2C_4 z} p_i^2 + \left(\frac{p_i^2 - p_o^2 e^{2C_4 L}}{e^{2C_4 L} - 1}\right)\left(e^{-2C_4 z} - 1\right)} \tag{47}$$

Thus, by substituting $C_4 = \frac{g sin\alpha}{\nu^2}$, we get the pressure distribution along the spatial coordinate z

$$p = \sqrt{e^{-2\frac{g sin\alpha}{\nu^2} z} p_i^2 + \left(\frac{p_i^2 - p_o^2 e^{2\frac{g sin\alpha}{\nu^2} L}}{e^{2\frac{g sin\alpha}{\nu^2} L} - 1}\right)\left(e^{-2\frac{g sin\alpha}{\nu^2} z} - 1\right)} \tag{48}$$

The two key equations (37)-(48) provide the value of mass-flow rate and pressure distribution for given physical parameters of the pipe, including nonzero inclination angle. Similarly to the previous zero-angle case, numerous relations can be derived from these equations. For example, you can specify the condition (40) for choking the pipeline.

C. Solutions Convergence

For validation purposes, it is vital to check the convergence of the analytic solution for $\alpha \neq 0$ to the case of $\alpha = 0$. We need to consider both the flowrate and the pressure distribution.

Flowrate. The limiting case of (35) for $\alpha \to 0$ ($C_4 \to 0$):

$$\lim_{C_4 \to 0} q|q| = \frac{2DA^2}{\lambda \nu^2} \lim_{C_4 \to 0} C_4 \left(\frac{p_i^2 - p_o^2 e^{2C_4 L}}{e^{2C_4 L} - 1}\right) \tag{49}$$

can be shown as

$$\lim_{C_4 \to 0} q|q| = \frac{2DA^2}{\lambda \nu^2} \lim_{C_4 \to 0} \eta(C_4) \cdot \lim_{C_4 \to 0} \left(p_i^2 - p_o^2 e^{2C_4 L}\right) \tag{50}$$

where $\eta(x) = \frac{x}{e^{Kx} - 1}$. According to (60), proved in Appendix, there exists a limit for η which is equal to $\frac{1}{2L}$. This leads you to

$$\lim_{C_4 \to 0} q|q| = \frac{2DA^2}{\lambda \nu^2} \frac{p_i^2 - p_o^2}{2L} \tag{51}$$

which is equal to (17) and concludes the proof of the (mass) flowrate convergence.

Mass flow as a function of pipe length L for different inclination angles is shown in Fig. 2. As can be computed from (40), with $\alpha = 3°$ the clog effect ($q = 0$) occurs for L about 40 km, and with $\alpha = 15°$ this effect appears at the distance L of about 8 km. Note that negative values of the mass-flow are attributed to the fact that in such operation points the fluid will flow in the opposite direction.

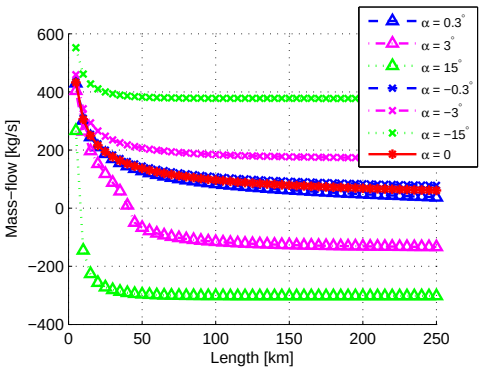

Fig. 2. Mass flow for different inclination angles as a function of pipeline length L computed for the following experimental setting: $p_i = 10$ MPa, $p_o = 8$ MPa, $\nu = 304\ \frac{m}{s}$, $g = 9.81\ \frac{m}{s^2}$, $D = 0.6$ m, $\lambda = 0.02$

Pressure distribution. Expression (46) in the limit $C_4 \to 0$ gets the following forms:

$$\lim_{C_4 \to 0} p^2 = \lim_{C_4 \to 0}\left(e^{-2C_4 z} p_i^2 + \left(\frac{p_i^2 - p_o^2 e^{2C_4 L}}{e^{2C_4 L} - 1}\right)\left(e^{-2C_4 z} - 1\right)\right) \tag{52}$$

$$\lim_{C_4 \to 0} p^2 = p_i^2 + \lim_{C_4 \to 0}\left[\left(\frac{p_i^2 - p_o^2 e^{2C_4 L}}{e^{2C_4 L} - 1}\right)\left(e^{-2C_4 z} - 1\right)\right] \tag{53}$$

which lead to

$$\lim_{C_4 \to 0} p^2 = p_i^2 + \lim_{C_4 \to 0}\left(p_i^2 - p_o^2 e^{2C_4 L}\right) \lim_{C_4 \to 0} \tilde{\eta}(C_4) \tag{54}$$

where $\tilde{\eta}(x) = \frac{e^{K_1 x} - 1}{e^{K_2 x} - 1}$. According to the derivation of (61), there exists a limit for $\tilde{\eta}$ equal to $\frac{-z}{L}$. Therefore, we have

$$\lim_{C_4 \to 0} p^2 = p_i^2 - \frac{z}{L}\left(p_i^2 - p_o^2\right) \tag{55}$$

which is equivalent to (19), and concludes the proof of the pressure convergence. Pressure distribution is illustrated in Fig. 3 for different inclination angles.

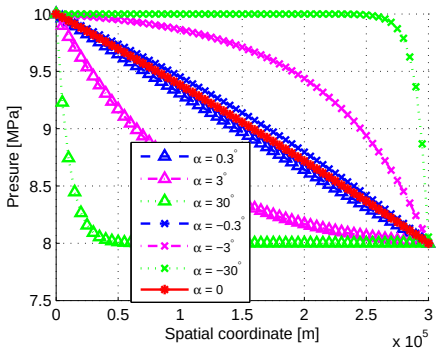

Fig. 3. Distribution of pressure along the pipeline for different inclination angles, in the experimental setting defined by: $p_i = 10$ MPa, $p_o = 8$ MPa, $\nu = 304\ \frac{m}{s}$, $D = 0.6$ m, $g = 9.81\ \frac{m}{s^2}$, $L = 75000$ m

Note also that for the case with the inclination angle equal to 30°, the highest drop of the pressure occurs at the beginning of the pipe, while for the case of negative inclination – the highest pressure drop is near the outlet of the pipe. Such considerations may be helpful in adjusting the pipe wall thickness to pressure.

IV. Exemplary Applications of the Model

The derived model provides an analytic connection between the most essential parameters of the flow. Thus, it constitutes a powerful tool for a pipeline engineer. Here we present some examples how it could be used.

A. Exemplary Relationships

First we apply the obtained model (35) to determine the resulting flowrate for the given physical pipeline parameters and the given input and output pressure. A 3D plot presenting the dependency of the flowrate on the inlet and outlet pressure for an exemplary pipeline is shown in Fig. 4. This plot expresses

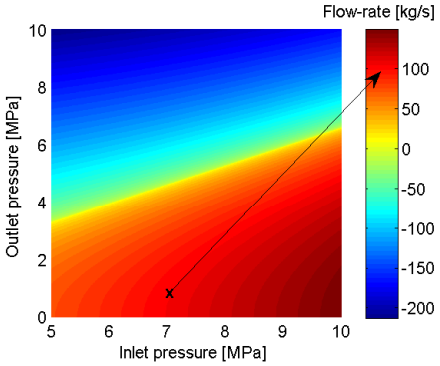

Fig. 4. Distribution of the flowrate, as dependent on the pressure at both ends of the pipeline, with the experimental setting defined by: $\nu = 304\ \frac{m}{s}$, $g = 9.81\ \frac{m}{s^2}$, $L = 75000$ m, $\lambda = 0.02$, $d = 0.6$ m, $\alpha = 3^\circ$

the most essential information about the flow resulting from the selected pair of inlet and outlet pressures. It can be helpful, for instance, when one wants to transport a specific amount of fluid over time, and have to select pumping pressures. You can indicate a curve describing the pressure combination to provide the desired flowrate. In particular, a zero flow curve can be indicated which determines the minimum inlet pressure (for the given outlet pressure) so that the flow occurs. Clearly, negative flowrates mean that the fluid flows in the opposite direction.

Another application can be found in designing the diameter of the pipe, suitable for the desired pipeline operation (in terms of pressure and flowrate). Due to the limited length of this article, this example will not be discussed in more detail here. Of course, these are just examples of the use of the developed model. Though this is a difficult, multidimensional relationship, selected relationships and combinations of parameters can still be conveniently represented as 2D or 3D charts.

B. Comparison of the Numeric and Analytic Approaches

The model allows to simulate a straight pipeline with zero or non-zero inclination angle. The following experiment shows the error (with respect to N-section numerical simulation) when the model is applied for a pipeline consisting of few pieces with different inclination angle. In our experiment we consider a pipeline of the total length of 75 km, constructed of five equally long pieces. Three pieces arts (boundary and middle) have the inclination angle equal to 0, and the other two have the inclination angle α engineered as a parameter. A diagram of this pipeline is presented in the Fig. 5. Two

TABLE I
Computation times for varying N

Number of segments	Time [s]	Time [min]	Time [h]
Analytic model	$7.25 \cdot 10^{-6}$	$1.21 \cdot 10^{-7}$	$2 \cdot 10^{-9}$
20	0.14	$2.4 \cdot 10^{-3}$	$3.9 \cdot 10^{-5}$
40	0.18	$3 \cdot 10^{-3}$	$5 \cdot 10^{-5}$
80	3.11	$5.2 \cdot 10^{-2}$	$8.6 \cdot 10^{-4}$
160	91	1.52	$2.5 \cdot 10^{-2}$
320	$1.3 \cdot 10^{3}$	21	0.35
640	$2 \cdot 10^{4}$	336	5.59

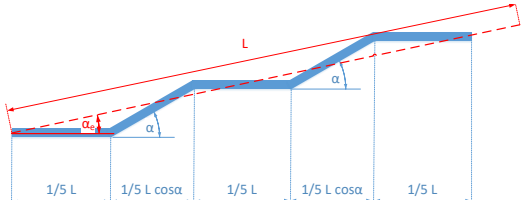

Fig. 5. Dimensioning of the pipeline considered in full-blown simulation (with the use of α), and the effective angle α_e used in the analytic solution (marked by the dash line)

models were implemented for the variable inclination angle: the state-base dynamic simulation model (6) and the aggregate analytic solution (37) for $\alpha = \alpha_e$, and (18) for $\alpha_e = 0$. The resulting computing error of the flow rate as a function of the inclination angle is shown in Fig. 6, for various segmentation.

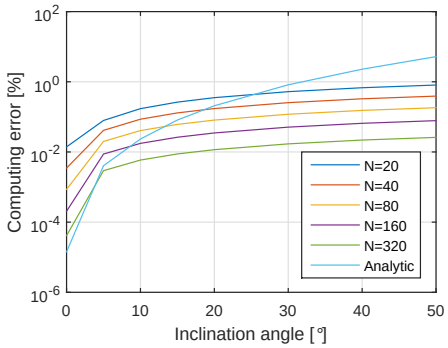

Fig. 6. Relative flowrate errors for differently (N-section)simulated pipelines and the analytic solution, all for varying inclination angle in the following experimental setting: $p_i = 8$ MPa, $p_o = 7$ MPa, $\nu = 300\ \frac{m}{s}$, $g = 9.81\ \frac{m}{s^2}$, $L = 6000$ m, $d = 0.67$ m, $\lambda = 0.02$

For the zero inclination angle, the relative error decreases as the number of simulation segments (N) increases. One can see that, for zero inclination, numerical simulation is convergent to the analytic solution. As the angle increases, or we have a complex structure of the pipeline, numerical simulation can be, in general, more suitable. In particular, up to 16° the

analytic solution, using merely the straight pipe model and a single equation, leads to results comparable with the most precise simulations ($N = 80, 160, 320$), using the assumed irregular shape. Note, however, the high computational costs of simulation, where the numerical solution for steady-state is obtained through numerous iterations of the simulation algorithm, which in the case of 640 segments takes almost 6 hours for a 2.8 GHz 4-core CPU as shown in Tab. I.

V. Conclusion

The issue of modeling the flow process in transmission pipelines has been addressed. A base model used for numerical simulation has been first introduced. Under a certain assumption regarding the steady state analysis, the two differential equations are solved for two cases: zero and nonzero inclination angle. As a result we have obtained the formulas for the constant flow rate and the distribution of the pressure along the considered pipeline for both cases. A useful relationship between the inclination angle, pipe length, and zero-flow pressure, has been given. Convergence of the derived analytic solutions for the inclination angle $\alpha \to 0$ has also been shown. Exemplary applications of the obtained model have been considered. For instance, a 3D plot presenting the relationship of flow-rates on inlet and outlet pressures (useful in operation of pipelines) has been given. A test pipeline with partly adjustable inclination angle has been considered in an experimental study. The experiment has shown that the numerical solution is convergent to the analytic one for slightly slanted pipes. Moreover, it has been proved that even for differently shaped pipes and up to 16°, the analytic solution (using the effective angle) makes a sufficient approximation (the relative error less than 1% or 1‰).

Appendix: Limit Case of $\eta(x)$ and $\tilde{\eta}(x)$

By performing the Taylor expansion of the exponent around the point 0 with respect to the variable x:

$$e^{Kx} = 1 + \frac{Kx}{1!} + \frac{(Kx)^2}{2!} + \frac{(Kx)^3}{3!} + \dots \tag{56}$$

for a constant K, and by considering $e^{Kx} - 1$ as

$$e^{Kx} - 1 = \frac{Kx}{1!} + \frac{(Kx)^2}{2!} + \frac{(Kx)^3}{3!} + \dots \tag{57}$$

the $\eta(x)$ can be easily shown as

$$\eta(x) = \frac{x}{e^{Kx} - 1} = \frac{x}{Kx + \frac{(Kx)^2}{2!} + \frac{(Kx)^3}{3!} + \dots} \tag{58}$$

and, finally

$$\eta(x) = \frac{1}{K + \frac{K^2 x}{2!} + \frac{K^3 x^2}{3!} + \dots} \tag{59}$$

Hence, the limit for $x \to 0$ is

$$\lim_{x\to 0} \frac{x}{e^{Kx} - 1} = \lim_{x\to 0} \frac{1}{K + \frac{K^2 x}{2!} + \frac{K^3 x^2}{3!} + \dots} = \frac{1}{K} \tag{60}$$

Note that K can be both positive and negative.

In an analogy to (60), we can calculate $\tilde{\eta}(x)$ as

$$\tilde{\eta}(x) = \lim_{x\to 0} \frac{e^{K_1 x} - 1}{e^{K_2 x} - 1} = \\ = \lim_{x\to 0} \frac{\frac{K_1 x}{1!} + \frac{(K_1 x)^2}{2!} + \frac{(K_1 x)^3}{3!} + \dots}{\frac{K_2 x}{1!} + \frac{(K_2 x)^2}{2!} + \frac{(K_2 x)^3}{3!} + \dots} = \frac{K_1}{K_2} \tag{61}$$

References

[1] L. Billmann and R. Isermann: *Leak detection methods for pipelines*, Automatica, 23(3), 381-385, 1987.

[2] J.A. Delgado-Aguiñaga, G. Besançon, O. Begovich and J.E. Carvajal, *Multi-leak diagnosis in pipelines based on Extended Kalman Filter*, Control Engineering Practice, Volume 49, p. 139-148, ISSN 0967-0661, http://dx.doi.org/10.1016/j.conengprac.2015.10.008, 2016.

[3] K. Gunawickrama, *Leak detection methods for transmission pipelines*, (PhD Thesis supervised by Z. Kowalczuk). Gdansk University of Technology, Gdańsk, 2001.

[4] Z. Kowalczuk and K. Gunawickrama, *Detection and localization of leaks in transmission pipelines*, In Korbicz, J., Kościelny J.M., Kowalczuk, Z., Cholewa, W. (Eds.): Fault Diagnosis. Models, Artificial Intelligence, Applications, pp. 821-864. Springer, Berlin, Heidelberg, New York, 2004.

[5] Z. Kowalczuk and M. Tatara, *Analytical modeling of flow processes: Analysis of computability of a state-space model*, In XI Int. Conf. on Diagnostics of Processes and Systems, 8-11 September 2013, pages 74.1-12. Łagów Lubuski, 2013.

[6] Z. Kowalczuk and M. Tatara, *Approximate models and parameter analysis of the flow process in transmission pipelines*, In Kowalczuk Z. (Ed.): Advanced and Intelligent Computations in Diagnosis and Control, vol. AISC 386, pp. 209-220. Springer IP Switzerland [ISBN 978-3-319-23180-8 (eBook); DOI 10.1007/978-3-319-23180-8_17], Cham, Heidelberg, New York, Dordrecht, London, 2016.

[7] Z. Kowalczuk and M. Tatara, *Numerical issues and approximated models for the diagnosis of transmission pipelines*, In Advances in the Diagnosis of Faults in Pipeline Networks, pp. 1-24. Springer, Berlin, Heidelberg, 2017.

[8] Z. Kowalczuk, M. Tatara and T. Stefański, *Reduction of Computational Complexity in Simulations of the Flow Process in Transmission Pipelines*, In XIII Int. Conf. on Diagnostics of Processes and Systems, 10-13 September 2017, Poland, Sandomierz, 2017.

[9] S. Li, Y. Wen, P. Li, J. Yang, X. Dong and Y. Mu, *Leak location in gas pipelines using cross-time-frequency spectrum of leakage-induced acoustic vibrations*, Journal of Sound and Vibration, 333(17), 3889-3903. https://doi.org/10.1016/j.jsv.2014.04.018, 2014.

[10] S. Li, J. Zhang, D. Yan, P. Wang, Q. Huang, X. Zhao, Y. Cheng, Q. Zhou, N. Xiang and T. Dong, T., *Leak detection and location in gas pipelines by extraction of cross spectrum of single non-dispersive guided wave modes*, Journal of Loss Prevention in the Process Industries, 44, 255-262. https://doi.org/10.1016/j.jlp.2016.09.021, 2016.

[11] S.K. Mandal, F.T.S. Chan, and M.K. Tiwari, *Leak detection of pipeline: An integrated approach of rough set theory and artificial bee colony trained SVM*, Expert Systems with Applications, 39(3), 3071-3080. https://doi.org/10.1016/j.eswa.2011.08.170, 2012.

[12] P. Ostapkowicz and A. Bratek, *Leak detection in liquid transmission pipelines during transient state related to a change of operating point*, In: Kowalczuk Z (Ed.) Advanced and Intelligent Computations in Diagnosis and Control, vol. AISC 386, pp. 253-265. Springer IP Switzerland [ISBN 978-3-319-23180-8 (eBook)], Cham, Heidelberg, New York, Dordrecht, London, 2016.

[13] C. Verde, N. Visairo and S. Gentil, *Two leaks isolation in a pipeline by transient response*, Advances in Water Resources, vol. 30, issue 8, pp. 1711-1721, ISSN 0309-1708, 2007.

[14] C. Verde and L. Torres, *Referenced model based observers for leaks' location in a branched pipeline*, The 9th International Federation of Automatic Control (IFAC) Symposium SAFEPROCESS-2015, Paris, France, 2015.